

Received May 23, 2021, accepted June 8, 2021, date of publication June 14, 2021, date of current version June 22, 2021.

Digital Object Identifier 10.1109/ACCESS.2021.3089251

# A Method for Constructing Automatic Rolling Bearing Fault Identification Model Based on Refined Composite Multi-Scale Dispersion Entropy

QINGFENG WANG<sup>1,2</sup>, YANG XIAO<sup>1,2</sup>, SHUAI WANG<sup>1,2</sup>, WENCAI LIU<sup>3</sup>, AND XIAOJIN LIU<sup>1,2</sup>

<sup>1</sup>Beijing Key Laboratory of Health Monitoring and Self-Recovery of High-End Machinery Equipment, Beijing University of Chemical Technology, Beijing 100029, China

<sup>2</sup>Diagnosis and Self-Recovery Engineering Research Center, Beijing University of Chemical Technology, Beijing 100029, China

<sup>3</sup>CNPC Research Institute of Safety and Environment Technology, Beijing 102206, China

Corresponding author: Qingfeng Wang (wangqf2422@buct.edu.cn)

This work was supported in part by the Key Projects of CNPC Research Institute of Safety and Environment Technology under Grant AY2019 Safety/Reception (Research) 004, and in part by the Joint Project of BRC-BC under Grant XK2020-04.

**ABSTRACT** In this paper, one of most widely utilized rolling bearings in rotating machinery is selected as the research object. Automatic rolling bearing fault identification model including support vector machine (SVM) training module, fault classification knowledge base module, and fault automatic identification module is proposed. A generalized method for automatic identification of rolling bearing faults based on refined composite multi-scale dispersion entropy (RCMDE) is developed. First, in order to solve the problem of setting the value range of the decomposition level  $K$  based on empirical knowledge for variational modal decomposition (VMD), a maximum kurtosis value method is proposed to determine the preset value range of  $K$  in whale optimization algorithm. Then, an improved VMD method is used to adaptively decompose the signal into a series of intrinsic mode function components. Next, the correlation coefficient method is employed to screen effective feature components of bearings in different health states for reconstruction. Through theoretical analysis, the calculated RCMDE value of reconstructed signal is screened and input as a feature value into the optimized SVM classifier for fault pattern recognition. The input of rolling bearing vibration data without preprocessing and the output of the fault identification which don't rely on empirical knowledge of external experts is realized. Experimental and engineering case data of rolling bearings under different equipment and operating environments are tested and validated. The results indicate that the model proposed in this paper shows good fault identification, demonstrates good generalization performance, and has beneficial industrial application prospect.

**INDEX TERMS** Refined composite multi-scale dispersion entropy, generalization, automatic fault identification, variational modal decomposition, support vector machine.

## I. INTRODUCTION

In Industry 4.0, traditional refining and chemical integrated production equipment are facing digital transformation and upgrading. Once an unplanned shutdown accident of key component in a process industry production device occurs, it may cause drastic production losses and disastrous environmental consequences [1]. Breakdown maintenance (BM), time-based maintenance (TBM), and condition-based

maintenance (CBM) that rely on external experts to carry out fault diagnosis and analysis have difficulties meeting the requirements of equipment safety, reliability, long-term stability, and cost-effective operation. Predictive maintenance (PdM) is an emerging maintenance method, which not only evaluates the current operating status of the equipment, but also diagnoses its future cracking trends and failures [2]. It includes the following five basic contents: early detection of equipment performance degradation, health status assessment, automatic failure mode identification, operation status trend prediction, and maintenance strategy formulation [3].

The associate editor coordinating the review of this manuscript and approving it for publication was Mehrdad Saif<sup>1</sup>.

Failure pattern recognition, which serves as an intermediate link, is a very important PdM part.

Gas turbine is the very important power machinery in petrochemical, aviation and other industrial systems, and rolling bearings are one of the most widely employed components in gas turbines such as aeroengines [4]. Once they fail, the operating status of the entire mechanical equipment is directly affected [5], [6]. Therefore, in-depth study of failure mode recognition PdM technology of rolling bearings and timely identification of their incipient fault is important for ensuring the safe operation of equipment. In recent years, application of pattern recognition method theory in fault diagnosis of rotating machinery equipment has been very common. Time-frequency domain analysis [7], expert system [8], neural network [9], sparsity indexes [10], adaptive encoder [11] and other methods have been consistently used for fault diagnosis of rolling bearings. Bearing fault diagnosis method is based on inner product continuation local mean decomposition and support vector machine (SVM) [12]. Online fault analysis method is based on improved multi-scale fuzzy entropy [13], while intelligent fault identification is based on relatively big data software and parallel machine learning algorithms [14]. Another example of diagnosis method is the fault diagnosis method founded on noise reduction technology and improved convolutional neural network (CNN) [15]. However, many failure mode recognition methods and condition monitoring systems based on time-frequency domain analysis and deep learning are also dependent on theoretical knowledge of external experts. Furthermore, these methods have not yet been able to achieve automatic failure mode recognition based on the “black box” theory. In addition, the existing fault recognition models proposed by researchers have poor generalization and are often difficult to apply in industry.

Variational modal decomposition (VMD) is an adaptive and completely non-recursive method of modal variation and signal processing [16], which can effectively reduce the noise of the actual vibration signals of rolling bearings in industrial applications. However, VMD also exhibits some drawbacks. For example, the selection of decomposition level  $K$  and penalty factor  $\alpha$  depends on empirical knowledge. To ensure more reasonable selection of parameters, Song *et al.* [17] studied an optimized VMD mode number  $K$  screening method. The parameter  $K$  was reasonably set, de-noising signal was decomposed into multiple characteristic modal components, and optimal characteristic modal component was screened according to the kurtosis value. Hence, excessive signal decomposition was avoided and loss of effective information from vibration signals was reduced. However, the authors did not optimize the value of the penalty factor  $\alpha$ . In order to avoid deviation of the results caused by separate optimization of penalty factor  $\alpha$  and decomposition level  $K$ , Ding *et al.* [18] proposed a VMD method based on genetic mutation particle swarm optimization. Within the method, parameters were optimized through generalized particle swarm algorithm. Genetic mutation

particle swarm optimization VMD method has better decomposition effect and fault diagnosis accuracy when compared with the fixed parameter VMD algorithm. However, this method does not filter the intrinsic mode function (IMF) components after decomposition, and the effectiveness of the reconstruction order is difficult to guarantee. To screen an effective reconstruction order, Wang *et al.* [19] proposed a VMD method based on adaptive parameter optimization. The method automatically screens the effective reconstruction order based on a singular kurtosis difference spectrum. Optimal parameter combination of the center frequency ratio of two adjacent modes to the threshold was compared. However, automatically selecting effective reconstruction order differs significantly in convergence accuracy of different vibration signals. In order to solve low convergence accuracy problem in parameter optimization of penalty factor  $\alpha$  and decomposition level  $K$ , Li *et al.* [20] proposed a combination of wavelet threshold de-noising, VMD genetic algorithm optimization, and whale optimization algorithm (WOA) of least squares support vector machine method (LSSVM). However, eigenvalue wavelet packet energy entropy lacked the ability to characterize bearing fault characteristics when exposed to various equipment conditions, with relatively weak corresponding generalization present.

In fact, feature extraction directly affects fault diagnosis results [4]. With ever increasing of the need of fault diagnosis accuracy, multi-scale analysis can reflect the complexity of vibration signal and obtain more characteristic signal information, so it has often been utilized in the field of fault diagnosis [21], [22]. Han *et al.* [23] proposed a fault diagnosis algorithm based on improved deep belief network. Within the method, wavelet packet energy entropy and multi-scale permutation entropy (MPE) combined with the feature matrix were employed to classify deep features. Li *et al.* [24] proposed a signal processing scheme for the selection of scale factors. Improved Vold-Kalman filter and multi-scale sample entropy (MSE) were combined to screen scale factors for non-stationary work. In planetary gearbox fault diagnosis, this method was proven as superior when compared to the ensemble empirical mode decomposition (EEMD)-MSE fault diagnosis method. Even though MPE and MSE analysis methods are effective in fault identification, they have some inevitable disadvantages. Although MPE method requires relatively simple calculation, it does not consider amplitude relationship between the signals. With an increase in the scale factor, coarse-grained process of time series causes a loss of characteristic information of the vibration signal at a larger scale [25]. The MSE method has a slow calculation speed for long-period data poor effect on real-time signals and abrupt signal processing.

To offset the shortcomings of MPE and MSE methods, Rostaghi and Azami [26] proposed a new measurement index algorithm—dispersed entropy (DE). Based on simulated linear and biological signals, DE, PE, and SE algorithms are mutually compared. The results indicate that DE method has better stability and faster calculation speed when compared

to PE and SE algorithms. Azami *et al.* [27] proposed refined composite multi-scale dispersion entropy (RCMDE) method. The results, which were obtained by comparing with several other multi-scale methods, indicated that RCMDE method has relatively small calculation error and excellent feature extraction effect when processing long signals. Zhang *et al.* [28] proposed a rolling bearing fault diagnosis method based on RCMDE and improved support vector machine. The effectiveness of this method was experimentally validated. Zheng *et al.* [29] proposed a rolling bearing fault diagnosis method based on improved empirical wavelet transform (IEWT) and RCMDE. The proposed method can accurately distinguish rolling bearing failure types and has high fault diagnosis accuracy.

If RCMDE directly acts on the original signal, it cannot accurately reveal inherent vibration signal characteristics. When type and severity of bearing faults are different, only RCMDE is used for fault diagnosis, which may not produce ideal results [30]. It is necessary to overcome the nonlinear characteristics of actual engineering vibration signal and improve the accuracy of diagnosis. Fei *et al.* [31] proposed an optimized generalized regression neural network to solve the nonlinear problem of multi-body flexible mechanism modeling. Feng *et al.* [32] proposed an interval dynamic matrix with additional margin method to control the nonlinear speed change of pipeline inner detector. Fei *et al.* [33] proposed an improving support vector regression method to be applied to turbine of nonlinear material parameters. In addition, SVM classifier based on RBF kernel function can also solve the nonlinear problem well, so it is widely employed in the field of fault diagnosis. Liu *et al.* [34] have proposed the method based on optimized SVM can effectively identify faults of the pumping well.

In response to the development trend of equipment PdM technology and the demand of practical engineering applications, a generalized automatic rolling bearing fault identification model based on RCMDE has been proposed and studied. In this paper, maximum kurtosis method is proposed to determine the preset range when WOA algorithm optimizes the  $K$  value, and then original vibration signal is de-noised and reconstructed based on improved VMD method. Finally, the extracted RCMDE feature values are screened and input into the optimized SVM for fault diagnosis. Experimental and engineering rolling bearing data under different equipment and operating environments are used to validate the model. The results indicate that the constructed model has a high rate of various rolling bearing faults identification and good generalization. The contribution of this paper can be summarized as follows:

(1) One RCMDE-based fault identification model has been constructed and a generalized method for constructing automatic rolling bearing fault identification model based on RCMDE is proposed.

(2) An optimization method for the preset value of the VMD decomposition level  $K$  is proposed. The problem that  $K$  value range presetting depending on human experience is

solved when applying WOA algorithm to optimize VMD, which can reasonably decompose the vibration signal of the rolling bearing and better characterize the fault characteristic information.

(3) Raw time series vibration data without preprocessing is used as the fault identification model input. Fault recognition accuracy can be automatically output, and automatic fault identification based on “black box” theory can be achieved without relying on empirical knowledge of external experts.

The remainder of this paper is structured as follows. In Section II, theoretical background is introduced. In Section III, construction, training, and verification methods of rolling bearing fault automatic identification model are introduced. In Section IV, rolling bearing experimental data, engineering case data, typical fault data (such as inner ring failure, outer ring failure, rolling element failure), and normal status data are employed to train and validate the automatic fault identification model. In Section V, the paper is summarized, and conclusions are given.

## II. THEORETICAL BACKGROUND

### A. IMPROVED VARIATIONAL MODAL DECOMPOSITION

VMD is a non-recursive signal decomposition method that can adaptively decompose the signal into discrete sub-bands  $u_k$ . The mode is sparse and pulsates tightly around the center frequency  $\omega_k$  [35]. The essence of the VMD method is to construct a variational problem which is as follows and solve it.

$$\begin{aligned} \min_{\{u_k\}, \{\omega_k\}} & \left\{ \sum_k \left\| \alpha_t \left[ (\delta(t) + \frac{j}{\pi t}) \cdot u_k(t) \right] e^{-j\omega_k t} \right\|_2^2 \right\} \\ \text{s.t.} & \sum_k u_k = f \end{aligned} \quad (1)$$

where  $\{u_k\}$  is a decomposed set of modal components,  $t$  is the time series,  $\delta$  is the Dirac distribution, and  $k$  is the decomposed set of center frequency components. The sum of all modal components is the signal  $f$ .

$$\begin{aligned} L(\{u_k\}, \{\omega_k\}, \lambda) & \\ = \alpha & \sum_{k=1}^K \left\| \alpha_t \left[ (\delta(t) + \frac{j}{\pi t}) \cdot u_k(t) \right] e^{-j\omega_k t} \right\|_2^2 \\ & + \left\| f(t) - \sum_{k=1}^K u_k(t) \right\|_2^2 + \left\langle \lambda(t), f(t) - \sum_{k=1}^K u_k(t) \right\rangle \end{aligned} \quad (2)$$

In Eq. (2), alternating direction method of multipliers is used to alternately update  $u_k^{n+1}$  and  $\omega_k^{n+1}$ . Through multiple iterations, minimum value in the Lagrange expression is found, i.e., the “saddle point” of the entire iteration process. Then, an optimal solution  $u_k(t)$  and  $\omega_k^{n+1}$  center frequency are obtained.

When VMD is used for signal decomposition, decomposition level  $K$  and penalty factor  $\alpha$  are often provided as empirical knowledge, which can easily cause information loss or over-decomposition problems [16]. The value of  $K$  affects decomposition results, and the smaller the value of

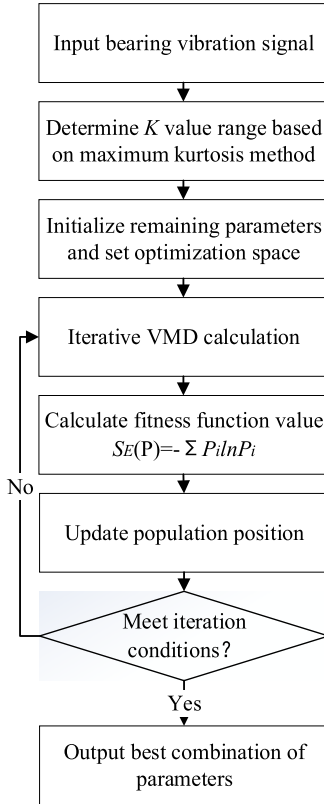


FIGURE 1. Flowchart of improved WOA method.

penalty factor  $\alpha$ , the larger the IMF bandwidth. As a new intelligent global simulation optimization algorithm, WOA has good global probability search capabilities [36], but it still need to set the initial range of parameters based on experience. To avoid the influence of human factors and automatically screen for the best combination, the maximum kurtosis method proposed in this paper is used to determine the preset range of the decomposition layer  $K$ , and can adaptively optimize parameters more accurately. Specific flowchart are as follows:

## B. FEATURE EXTRACTION

### 1) DISPERSION ENTROPY

DE is a nonlinear dynamic method that characterizes the complexity and irregularity of time series [26]. The calculation steps are as follows:

1) Nonlinear time series  $x\{x_1, x_2, \dots, x_N\}$  is mapped to  $y\{y_1, y_2, \dots, y_N\}$  through normal distribution function.

2) As shown in Eq. (3),  $y_i$  is mapped to  $z_i$  through linear transformation:

$$z_i = \text{int}(cy_i + 0.5) \quad (3)$$

3) As shown in Eq. (4), embedding vector  $z_i^{m,c}$  is calculated and mapped to the scatter pattern  $\pi_{v_0 v_1 \dots v_{m-1}}$ , where  $z_i^c = v_0, z_{i+d}^c = v_1, \dots, z_{i+(m-1)d}^c = v_{m-1}$ .

$$z_i^{m,c} = (z_i^c, z_{i+d}^c, \dots, z_{i+(m-1)d}^c), \quad i = 1, 2, \dots, N - (m-1)d \quad (4)$$

where  $m$  is the embedding dimension, and  $d$  is the time delay.

4) As shown in Eq. (5), the probability of each dispersion mode  $\pi_{v_0 v_1 \dots v_{m-1}}$  is calculated:

$$P(\pi_{v_0 v_1 \dots v_{m-1}}) = \frac{\text{num}(\pi_{v_0 v_1 \dots v_{m-1}})}{N - (m-1)d} \quad (5)$$

where  $\text{num}(\pi_{v_0 v_1 \dots v_{m-1}})$  is the number of  $z_i^{m,c}$  mapped to  $\pi_{v_0 v_1 \dots v_{m-1}}$ .

5) As shown in Eq. (6), DE value of a raw signal can be expressed as follows:

$$E_{DE} = - \sum_{\pi=1}^{c^m} P(\pi_{v_0 v_1 \dots v_{m-1}}) \ln(P(\pi_{v_0 v_1 \dots v_{m-1}})) \quad (6)$$

With an increase in DE value, degree of vibration signal irregularity is also increased. The same is applied for vice-versa.

### 2) REFINDE COMPOSITE MULTI-SCALE DISPERSION ENTROPY

RCMDE is a multi-scale method to the original signal, that is, equidistant division and then the average is calculate, further refinement on the basis of multi-scale dispersion entropy MDE [27]. When the RCMDE with a scale factor of  $\tau$  is calculated, first the original signal is divided into segments of length  $\tau$  continuously according to the initial points of  $[1, \tau]$ , then the average value of each segment is calculated, and then the average values are arranged in order as the coarse-grained sequence, a total of  $\tau$  coarse-grained sequences are obtained [29].

When the RCMDE value is calculated, the probability of the dispersion pattern of each coarse-grained sequence is calculated firstly, and then the average of these probabilities is calculated. This refined signal processing method can effectively reduce the loss of some statistical information during the coarse-graining process of the MDE algorithm. Multiple initial point positions are averaged, the influence of initial point positions on the calculation results can be effectively solved, and the calculation deviation can be reduced.

The RCMDE calculation steps are as follows:

1) As shown in Eq. (7), the raw data  $u$ 's  $k$ -th coarse-grained sequence  $x_k^{(\tau)} = \{x_{k,1}^{(\tau)}, x_{k,2}^{(\tau)}, \dots\}$  is given by:

$$x_{k,j}^{(\tau)} = \frac{1}{\tau} \sum_{b=k+\tau(j-1)}^{k+j\tau-1} u_b \quad j=1, 2, \dots, L/\tau \quad k=1, 2, \dots, \tau \quad (7)$$

2) The average value of the probability of the coarse-grained sequence in the scatter mode is defined as follows:

$$\bar{P}(\pi_{v_0 v_1 \dots v_{m-1}}) = \frac{1}{\tau} \sum_{k=1}^{\tau} P_k^{(t)} \quad (8)$$

3) In summary, the RCMDE value is defined as follow:

$$E_{RCMDE} = - \sum_{\pi=1}^{c^m} \bar{P}(\pi_{v_0 v_1 \dots v_{m-1}}) \ln(\bar{P}(\pi_{v_0 v_1 \dots v_{m-1}})) \quad (9)$$



**C. OPTIMIZED SUPPORT VECTOR MACHINE**

SVM is a machine learning algorithm based on statistical learning theory proposed by Cortes and Vapnik [37]. SVM has a relatively simple structure, good robustness, and strong generalization ability. It is based on assumption that a sample set  $\{(x_i, y_i), i = 1, 2, \dots, N\}$  exists. Within the sample set,  $x_i$  represents the input of the sample space,  $y_i$  represents the mapping value of  $x_i$ , and  $N$  is related to the size of the sample data. The input data vector is mapped to a high-dimensional feature space. As shown in Eq. (10), a linear regression of the feature space is obtained:

$$f(x) = [\omega^T, \phi(x)] + b \tag{10}$$

where  $\phi(x)$  is the mapping function of the high-dimensional feature space,  $\omega$  is the weight vector, and  $b$  is the offset vector.

As shown in Eq. (11), the best separation surface with the largest margin for binary classification is determined as:

$$\begin{cases} \min \frac{1}{2} \|\omega\|^2 \\ (\omega\phi(x_i) + b)y_i \geq 1 \end{cases} \tag{11}$$

where  $y_i$  the value of is -1 or +1. In order to improve the classification ability of SVM, slack variables  $\varepsilon$  and penalty factors  $C$  are introduced into Eq. (12):

$$\begin{cases} \min \frac{1}{2} \|\omega\|^2 + C \sum_{i=1}^l \varepsilon_i \\ (\omega\phi(x_i) + b)y_i \geq 1 - \varepsilon_i \end{cases} \tag{12}$$

As presented in Eq. (13), the Lagrange multiplier  $\alpha$  is increased:

$$\begin{cases} \max[\sum_{i=1}^l \alpha_i - \frac{1}{2} \sum_{i=1}^l \sum_{j=1}^l \alpha_i \alpha_j y_i y_j \phi(x_i) \phi(x_j)] \\ \sum_{i=1}^l y_i \alpha_i = 0 \end{cases} \tag{13}$$

Finally, optimal classification function is obtained:

$$\begin{cases} f(x) = \text{sgn}[\sum_{i=1}^m y_i \alpha_i K(x, x_i) + b] \\ K(x, x_i) = \exp(-\gamma \|x - x_i\|^2) \end{cases} \tag{14}$$

where  $m$  is the number of support vectors,  $K(x, x_i)$  is the kernel function equivalent, and  $\gamma$  is the kernel function bandwidth. In this paper, radial basis function (RBF) is chosen as the kernel function.

When RBF kernel is used to train SVM, two parameters critical to modelling must be considered: kernel function bandwidth and penalty factor [38]. Parameter  $\gamma$  affects training and prediction number. Parameter  $C$  affects the generalization ability of the model. In this paper, PSO algorithm is used to optimize these two parameters. The envelope spectrum is employed as the fitness function. It is observed that the model has the highest accuracy when envelope spectrum entropy is the smallest.

Basic theory of particle swarm optimization can be described as finding the optimal solution through collaboration and information sharing between group individuals. During iteration, individual extreme value is determined according to the fitness function value. Then, this value is shared with other particles. Finally, global extreme value is found. As shown in Eq. (19), speed and position of each particle is improved:

$$\begin{cases} v_{id}^{k+1} = \omega v_{id}^k + c_1 r_1 (p_{id}^k - x_{id}^k) + c_2 r_2 (p_{gd}^k - x_{id}^k) \\ x_{id}^{k+1} = x_{id}^k + v_{id}^{k+1} \end{cases} \tag{15}$$

where  $k$  is iterations at the current moment,  $d$  is current particle dimension,  $\omega$  is inertia weight.  $c_1$  and  $c_2$  are learning factors,  $r_1$  and  $r_2$  are random numbers.  $v_{id}^k$  and  $v_{id}^{k+1}$  are particle velocity at the current moment and particle velocity at the following moment.  $x_{id}^k$  and  $x_{id}^{k+1}$  represent particle position at the current moment and the following moment.  $p_{id}^k$  and  $p_{gd}^k$  represent local optimal value and global optimal value, respectively.

**III. CONSTRUCTION OF MODEL**

The main purpose of this paper is to use the raw data of rolling bearing normal state and three fault states, and generalized rolling bearing online fault automatic identification model is built.

As shown in Fig. 2, the orange solid box represents the improved VMD decomposition, IMF component screening, signal reconstruction, and RCMDE value calculation module in an offline training mode. The input data of this module is the normal state data and three types of labeled failure data of rolling bearing test bench. The output is four pattern recognition classification situations. The green area in the dotted frame represents online fault mode classification knowledge base. The dashed box is the online fault identification module in the online monitoring mode. Its input is real-time test data, and the output is the fault pattern recognition result.

**1) OFFLINE TRAINING MODE**

Step 1: Raw vibration signal rolling bearing data constitutes a training data set, which includes normal state data, inner ring fault data, outer ring fault data, and rolling element fault data. First, decomposition level  $K$  is determined according to the maximum kurtosis value. Then, penalty factor  $\alpha$  corresponding to the reconstructed signal is optimized via WOA. Next, correlation coefficient method is used to filter first three components with largest correlation coefficients for reconstruction. Finally, the RCMDE value of the reconstructed signal is calculated.

Step 2: Four types of fault feature vector spaces are established. Then, RCMDE values of four types of known label data which correspond to normal conditions, outer ring failure, inner ring failure, and rolling element failure, respectively, are calculated. Finally, following failure mechanism analysis, new failures that have not been yet identified can be added as a new category to form a failure mode classification knowledge base.

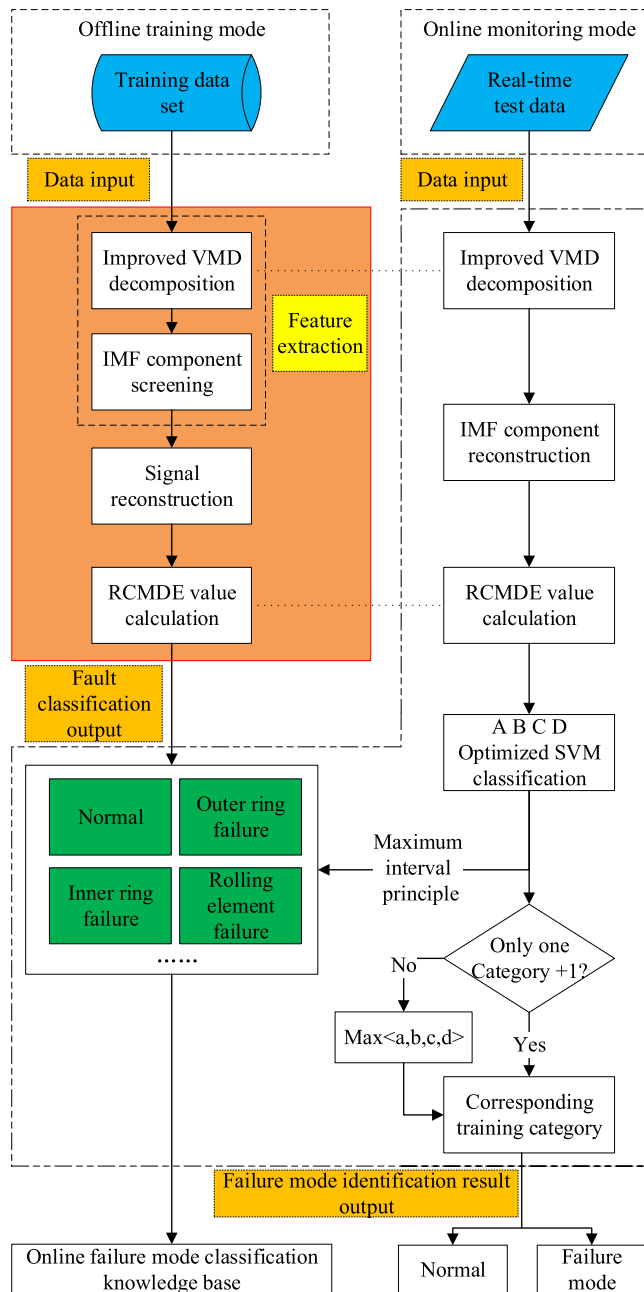


**FIGURE 2.** Framework diagram of RCMDE-based fault identification model.

## 2) ONLINE MONITORING MODE

Step 1: WOA algorithm is used to screen the real-time vibration signal penalty factor and decomposition level. Real-time vibration signal is decomposed to obtain  $K$  IMF components. Next, IMF components are filtered and reconstructed. Finally, RCMDE value of the reconstructed signal is calculated.

Step 2: RCMDE value is input into four optimized SVM classifiers A, B, C, and D to obtain four output results denoted as a, b, c, and d. Symbols A, B, C, and D correspond to normal state, outer ring failure, inner ring failure, and rolling element failure, respectively. The output result is compared with the fault knowledge base via maximum interval principle. If there

is only a single +1 type among the four results, it signals the corresponding failure mode. If there is more than one +1 type or there is no +1 type among the four results, failure mode corresponding to maximum a, b, c, or d is identified. Finally, the pattern recognition result is obtained as the output value.

## A. RAW SIGNAL DECOMPOSITION

The vibration signal contains information about the machine state. Improved VMD method is used to decompose bearing vibration signal into a series of modal components. VMD method reveals weak transient pulses from complex vibration signals, effectively suppresses modal aliasing, and has good noise robustness. WOA algorithm overcomes the problem of selecting VMD reasonable decomposition modulus. It can adaptively determine parameters  $K$  and  $\alpha$  for different bearing vibration signals. On the other hand, WOA cannot utilize the advantages of traditional VMD. However, it also has more generalization. According to the method proposed in this paper, decomposition level  $K$  is determined according to maximum kurtosis value. Then, penalty factor  $\alpha$  corresponding to the reconstructed signal is optimized through WOA. Parameter  $K$  is set as 2 or higher, and VMD decomposition is performed to obtain the maximum kurtosis of each decomposition. The maximum value of the kurtosis change curve is regarded as the optimal decomposition level. Based on the CWRU data, the method for determining the value of the decomposition level  $K$  of VMD is described as follows.

As shown in Fig. 3, first extreme point is obtained for  $K = 5$ , and maximum kurtosis decreases when  $K = 6$ . Then, maximum kurtosis increase is gradually lowered. If the value continues to increase, the calculation process is considered more complicated. Therefore, decomposition level is equal to  $K = 5$ . In order to meet the requirements of engineering data for different equipment and working conditions in practical applications, decomposition level in WOA algorithm is set from five to eight.

When VMD parameters are being optimized, the preset  $K$  value range is [5], [8] and the  $\alpha$  value range is [100,6000]. For bearing vibration signals, the WOA algorithm is used to multiple iterations within the preset value range. When the number of iterations reaches the set value and the fitness function converges,  $[K, \alpha]$  is output. The parameter combination  $[K, \alpha]$  can be determined adaptively by using different experimental data and engineering case data.

The vibration signal of each bearing group is decomposed into five levels of IMF components.

It can be seen from Fig. 4 and Fig. 5, time-domain waveform and VMD decomposition results of rolling bearings vibration signals in various states are as shown above.

## B. FEATURE COMPONENT SCREENING RULES

Since VMD frequency of each component is decomposed step by step from high to low frequency, correlation analysis between the natural frequency and raw vibration signal is employed in this section to screen sensitive characteristic

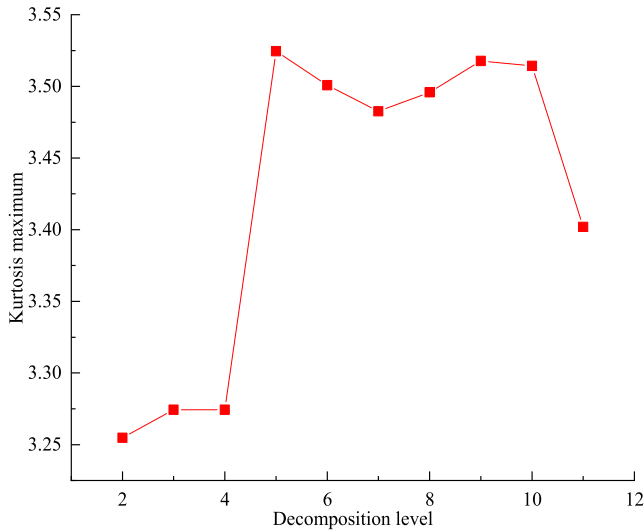


FIGURE 3. Variation of maximum kurtosis value with respect to decomposition layer.

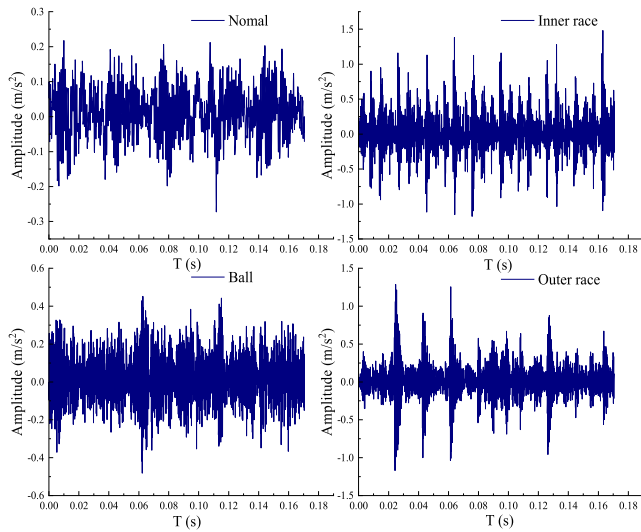


FIGURE 4. Time domain waveform.

components. The correlation coefficient  $r_{ci,x}$  between the  $i$ -th IMF component and its raw vibration signal is calculated according to Eq. (16):

$$r_{ci,x} = \left\| \frac{\sum_{i=1}^n (x(t) - \bar{x})(c_i(t) - \bar{c}_i)}{\sigma_{c_i}\sigma_x} \right\| \quad (16)$$

where  $x(t)$  is the original vibration signal,  $c_i(t)$  is the  $i$ -th IMF component of VMD decomposition,  $\sigma_{c_i}$  and  $\sigma_x$  are deviations of  $c_i$  and  $x(t)$ ,  $\bar{c}_i$  and  $\bar{x}$  are average values of  $c_i$  and  $x(t)$ .

Correlation coefficients of five IMF components obtained after decomposition of normal state and three fault states are calculated.

As shown in Fig. 6, the last three IMF components of the three fault states have larger correlation coefficients than the

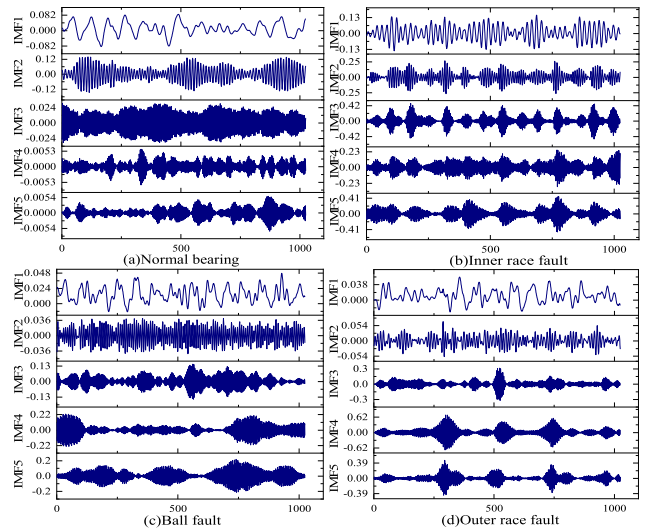


FIGURE 5. VMD decomposition results.

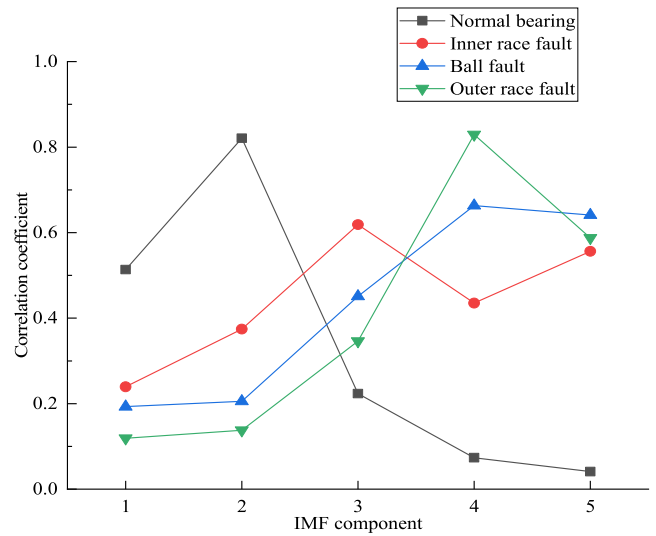


FIGURE 6. Correlation coefficient variation with respect to IMF component.

first two components. Correlation coefficients of first three IMF components in the normal state are relatively large, while fourth and fifth IMF components are relatively small. IMF component with small correlation coefficient is not highly correlated with the original signal. Moreover, less feature information is contained, which can be considered as insensitive feature components and filtered out.

Three IMF components with largest correlation coefficients of each bearing state of the sieve are calculated as sensitive feature components and reconstructed.

### C. FEATURE VECTOR CALCULATION

RCMDE value is related to embedding dimension  $m$ , category  $c$ , time delay  $d$ , and maximum scale factor  $\tau_{max}$ . When  $m$  is overly small, RCMDE value cannot be used to efficiently describe characteristics of the original signal. On the other

hand, if  $m$  is excessively large, RCMDE value is insensitive to signal fluctuations due to small RCMDE value. Therefore, value of  $m$  is generally taken as two or three. If  $c$  is relatively small, two different amplitudes may be assigned to the same category. If  $c$  is significantly large, a very small error may cause a change in its category. Hence, parameter  $c$  is taken within the range of [4], [8]. In addition, the time delay  $d$  is set to one. This is due to potential information loss when  $d$  is greater than one. The data length processed by RCMDE should be greater than 2000. In order to meet the application requirements of engineering data for different equipment and working conditions,  $\tau_{max}$  should not be too large [39]. Finally, in order to improve normal or fault bearing state characterization of RCMDE values, parameters in this paper are selected as:  $m = 3$ ,  $c = 6$ ,  $d = 1$ , and  $\tau_{max} = 15$ .

On most scales ( $\tau > 1$ ), rolling bearing vibration signals in four states can be clearly distinguished. Since normal state rolling bearing vibration is random, its vibration signal has a high degree of irregularity and low self-similarity. In failure state, regularity of rolling bearing vibration and self-similarity are both increased [40]. Therefore, RCMDE value of normal rolling bearing vibration signal is larger than the RCMDE value of three fault states. Normal rolling bearing vibration signal change trend of RCMDE value with the scale is different from the change trend of the fault signal. The overall RCMDE value trend of the faulty bearing vibration signal decreases with an increase in the scale factor. Moreover, the rate of decline also decreases with an increase in the scale factor. Although it rises on individual scales, it does not affect the overall downward trend. In this paper, RCMDE values of first five scales are selected as the sample feature vector. A classifier based on optimized SVM is used to classify these feature vectors and achieve fault pattern recognition of rolling bearings.

#### D. FAULT RECOGNITION CLASSIFICATION

Four fault source categories are employed within the method proposed in this paper. One-to-addition method is used to realize the multi-classification of rolling bearing fault identification. In other words, certain samples are classified into one category, and the remaining samples are classified into another category during training. Thus, samples of four categories construct four SVM classifiers. The SVM classifier maximizes the distance between the closest points of two category types via maximum interval principle. Therefore, hyperplane sample interval is maximized, and the classification is more accurate.

During model training, the  $i$ -th classifier takes the  $i$ -th type of data in the training set as positive samples. The remaining classes are divided into negative samples,  $i \in \{1, 2, 3, 4\}$ . When discriminating, the input signal passes through four classifiers to obtain a total of four output values,  $f_i(x) = \text{sgn}(g_i(x))$ . If only a single +1 value appears, its corresponding category is the input signal category, which represents an ideal situation. In actual situations, constructed decision function always has errors. If the output is more than

a single +1 value or none of the output is +1, the output values are mutually compared and category corresponding to the maximum value is denoted as the input signal category.

Bearing vibration signals are classified as follows: normal state and three fault states of the outer ring, inner ring, and rolling element correspond to four SVM classifiers A, B, C, and D, respectively. Part of the feature vector from each signal type is selected as the classifier training sample. The remaining feature vector is used as the classifier test sample. Corresponding training and test sample categories are created, and normal, outer ring, inner ring, and ball are marked with numbers 1, 2, 3, and 4, respectively. The training samples are placed into the classifier for training. Finally, the trained classifier is used to evaluate the test samples.

#### E. KNOWLEDGE BASE CONSTRUCTION

Raw vibration signal of the rolling bearing is screened. Then, model training is performed according to the above describe steps, and four classification results are obtained. Classifications 1, 2, 3, and 4 correspond to normal state, outer ring failure, inner ring failure, and rolling element failure, respectively. Based on the RCMDE value calculated from the rolling bearing vibration data, fault mode classification knowledge base corresponding to each bearing state is constructed.

Comprehensive consideration of sufficient rolling bearing failure case data and practical engineering experience, if fault identification accuracy of the real-time monitoring data is 85% or higher, current machine fault mode or normal operating state can be determined. If the fault recognition accuracy rate is below 85%, it is necessary to analyze the fault mechanism of the feature vector data set corresponding to the monitoring data. Accordingly, whether or not the machine belongs to other failure modes can be determined.

### IV. FAULT IDENTIFICATION MODEL AND DATA VERIFICATION

#### A. FAULT IDENTIFICATION MODEL

To validate the feasibility and recognition accuracy of the model, CWRU public rolling bearing failure data set is used for model training and process testing [41]. According to Fig. 7, CWRU test bench consists of an electric motor, a torque encoder, and a dynamometer *et al.* The sampling frequency of rolling bearings is 12 kHz, the bearing model is SKF 6205, and fault and sampling locations are both at the drive end of the bearing. The acquired vibration data set includes the bearing data in the normal state, inner ring failure, outer ring failure, and rolling element failure.

Based on the bearing speed and the sampling frequency of the sensor, it can be inferred that approximately 400 sampling points are collected for a single bearing revolution. As shown in Table 1, in order to ensure that the length of a single model test sample can completely and accurately record bearing vibration data in a specific health state, 2048 sampling points are taken as the length of a model test sample [42]. Under each workload operating environment, 30 sets of model training



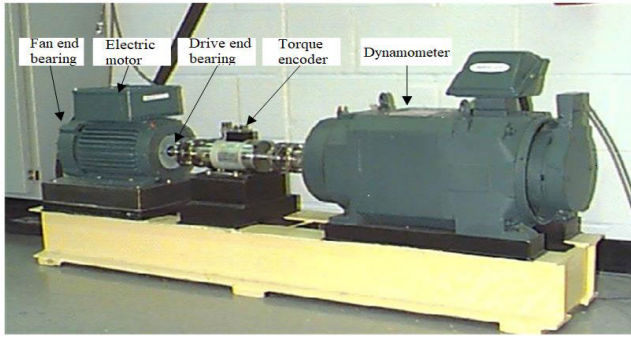


FIGURE 7. CWRU bearing test bench [41].

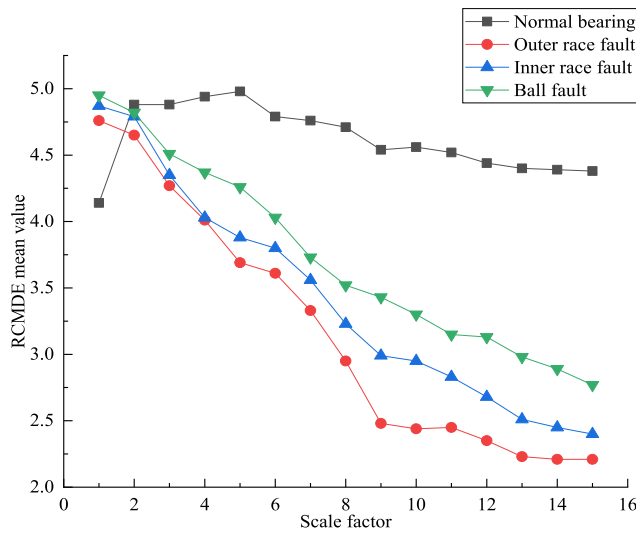


FIGURE 8. RCMDE mean value of bearing vibration signal.

samples are obtained for each bearing health state. Bearing vibration data of four CWRU health states and four working conditions are used as the training data set for cross-working and cross-device pattern recognition of the model. Each health state contains 120 sample sets, i.e., a total of 480 sample sets exist. The test set also screens other CWRU working condition data, experimental public data, and engineering case data.

For each set of bearing data, 30 sets of samples are selected, with the length of each set being 2048. RCMDE value of the reconstructed signal is then calculated. Average RCMDE value of different samples for each data type is shown in Fig. 8. On most scales ( $\tau > 1$ ), the entropy relationship of rolling bearing vibration signals in four states is  $E(NOR) > E(BRF) > E(IRF) > E(ORF)$ . If more scale RCMDE values are screened as the fault feature vector, information redundancy can occur and calculation time is greatly increased. Although the degree of discrimination between rolling bearings in different health states has increased to a certain extent, it is not conducive to classification and recognition in practical applications. However, if the number of the feature value is relatively small, faulty information may not be fully reflected, which decreases the recognition accuracy.

TABLE 1. Training data condition.

Label	Status	Fault Diameter (inch)	Number	Speed(r/min)
1	Normal bearing	0	30 × 4	1797 1772 1750 1730
2	Outer race fault	0.007	30 × 4	1797 1772 1750 1730
3	Inner race fault	0.007	30 × 4	1797 1772 1750 1730
4	Ball fault	0.007	30 × 4	1797 1772 1750 1730

TABLE 2. Test data condition.

Label	Status	Fault Diameter(inch)	Number	Speed(r/min)
1	Normal bearing	0	30	1797
2	Outer race fault	0.007 0.014 0.021	10 × 3	1797
3	Inner race fault	0.007 0.014 0.021	10 × 3	1797
4	Ball fault	0.007 0.014 0.021	10 × 3	1797

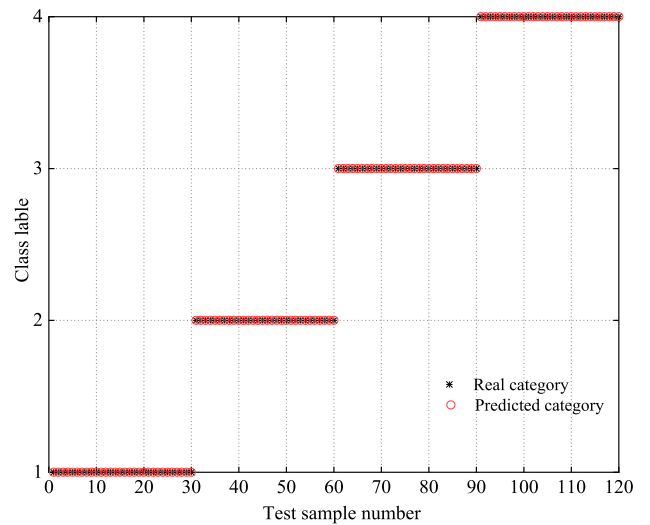


FIGURE 9. Test results of fault identification model based on CWRU experimental data.

RCMDE values of first five scales are selected as the training set feature vector and input into the SVM classifier.

SKF 6205 bearing data of the drive end with a sampling frequency of 48 kHz, speed of 1797 r/min. As shown in Table 2, outer race fault data, inner race fault data and ball fault data have been collection corresponding to the fault diameter of 0.007, 0.014 and 0.021 inch separately. Normal state, outer ring failure, inner ring failure, and rolling element failure contain 30 data groups each. Data length of a single group is 2048, and a total of 120 data groups are used as test sets. The result of parameters optimized by WOA algorithm is  $[K, \alpha] = [5, 2000]$ . The recognition accuracy of the test set is shown in Fig. 9.

As shown in Fig. 9, test set recognition accuracy is equal to 100%. The experiment is performed in 10-fold cross-validation with a standard deviation of 0. It shows that fault identification model based on CWRU data is very effective in identifying the same source data. All fault types can be accurately identified. The results indicate that the method proposed in this paper correctly identifies fault categories of rolling bearings. Furthermore, the method has a good vibration signal recognition effect when different sampling frequency is applied.

**B. VERIFICATION BASED ON EXPERIMENTAL DATA**

**1) IMS BEARING DATASET BASED MODEL VALIDATION**

Standard predicted vibration IMS data collected by the center for intelligent maintenance systems is employed. As shown in Fig. 10 [43], four Rexnord ZA-2115 double row bearings were installed on a shaft and forcibly lubricated. A spring mechanism was used to apply a radial load of 26689 N to bearings 2 and 3, while two high sensitivity PCB 353B33 Quartz ICP accelerometers were installed on each bearing along x and y axes. The rotation speed is kept constant at 2000 r/min by an AC motor connected to the shaft through a rubber belt. Lastly, sampling frequency of 20 kHz is employed.

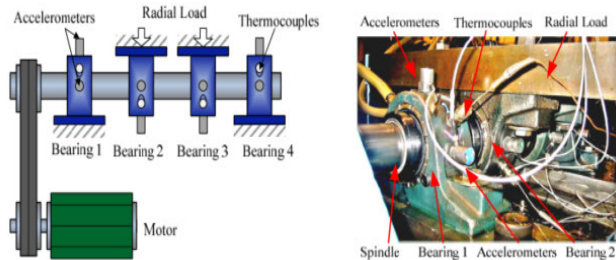


**FIGURE 10.** IMS test platform layout [43].

Three data set groups are included in IMS data. The second group of experimental bearings has four acquisition channels. The incipient fault detection method proposed by Wang et al. suggests that the fault occurred at 532<sup>nd</sup> data file [39]. The first channel is selected to collect the outer ring fault data after a fault occurs and to gather the normal data when no fault occurs. The first group of experimental bearings has eight acquisition channels. The sixth channel is used to collect the inner ring fault data, and the eighth channels are selected to collect the rolling element fault data. There are a total of 30 bearing data groups in every state, with 20480 data length for each group. RCMDE values of first five scales of the reconstructed signal are chosen as the test data. Then, the built model will be tested by the dataset. Based on the above data set, WOA algorithm can adaptively select the number of decomposition level as  $K = 5$  and penalty factor as  $\alpha = 1900$ .

As shown in Fig. 11, average RCMDE values of the first five scales of IMS data and CWRU data, which in normal state and rolling element failure are close, and data variation

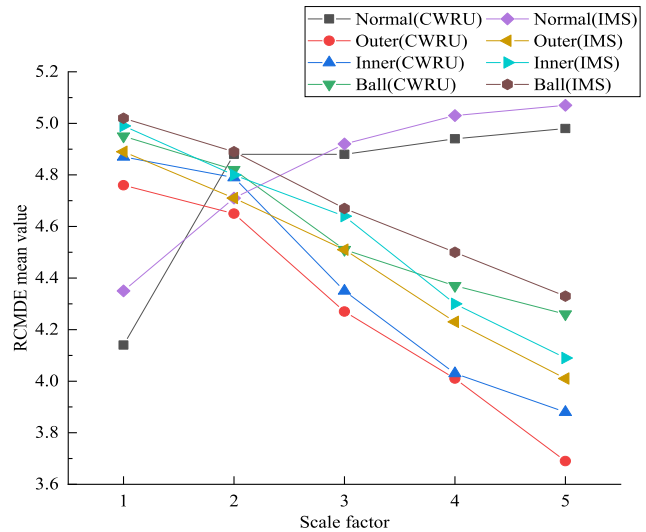


**FIGURE 11.** RCMDE mean value of CWRU data and IMS data.

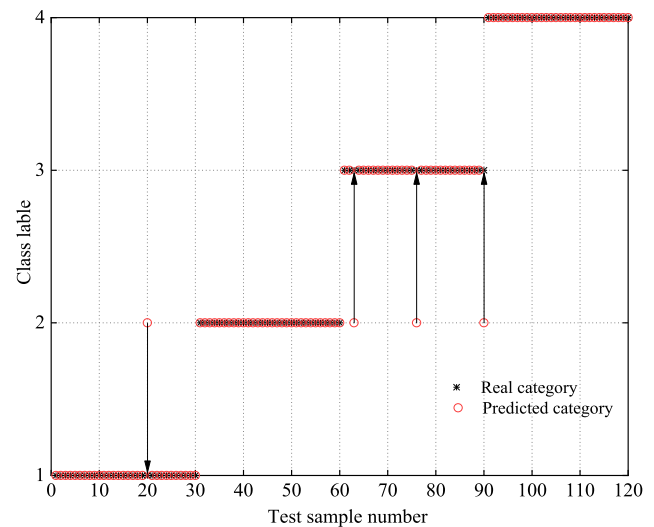


**FIGURE 12.** Test results of fault identification model based on IMS experimental data.

trend is basically identical, so the result of fault identification is good. For outer race fault data and inner race fault data, there is a little difference between two sets of data. RCMDE average value of IMS outer race fault data is closer to CWRU inner ring fault data, which will cause some fault data to be classified incorrectly.

As shown in Fig. 12, fault identification model based on CWRU data using RCMDE is also effective on IMS data. Three sets of inner ring fault data and one set of normal bearing data were incorrectly identified as the outer race fault. Thus, the recognition accuracy rate was 96.67%.

**2) MFPT BEARING DATASET BASED MODEL VALIDATION**

Experimental data sets provided by the Machinery Failure Prevention Technology (MFPT) are used for validation [44]. As shown in Table 3, rolling bearing data in the normal state, outer ring failure, and inner ring failure are selected as the

TABLE 3. MFPT bearing data parameters.

Label	Status	Load(lbs)	Sampling frequency	Sampling points
1	Normal bearing	270	97656	585936
2	Outer race fault	150 250 270	48828	146484
3	Inner race fault	100 200 300	48828	146484

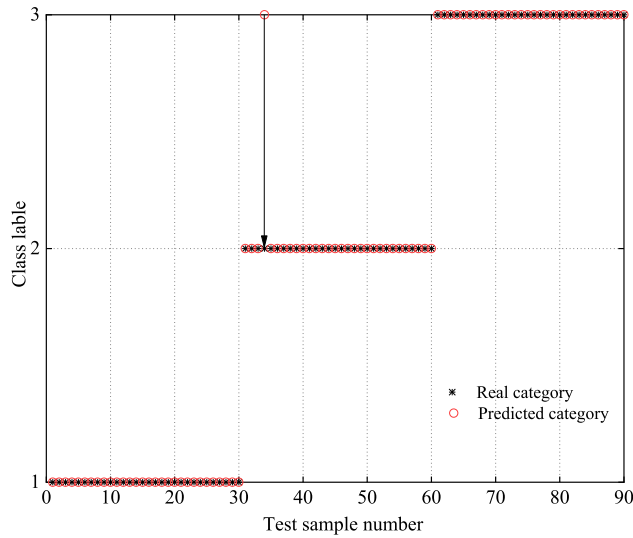


FIGURE 13. Test results of fault identification model based on MFPT experimental data.

test set data. Test data characteristics are described in detail as follows, and the continuous sampling time is three seconds.

For each type of health status data, 30 groups are screened. For outer ring fault data and inner ring fault data, there are 10 groups data set under three different load conditions have been gathered respectively. In total, 90 groups of test data with data length of 2048 are screened. According to adaptive adjustment of data via WOA algorithm, optimal result is obtained as [5, 3000]. Fault identification result is shown in Fig. 13.

MFPT data recognition accuracy rate is 98.9%, and only one set of outer ring fault data is incorrectly recognized. Laboratory data test results show that the bearing fault identification model proposed in this paper has a certain generalization. Moreover, it can accurately identify bearing vibration data of different speeds and loads. In order to verify the applicability of the proposed fault recognition model in an industrial environment, two sets of typical engineering case data are selected.

C. VERIFICATION BASED ON ENGINEERING DATA

1) 110P103B PUMP BEARING DATASET BASED MODEL VALIDATION

This data represents a case of free end bearing failure of a petrochemical company 110P103B pump. The layout of the pump bearing vibration monitoring points is shown in Fig. 14. The working speed of the pump is 1500 r/min, the bearing

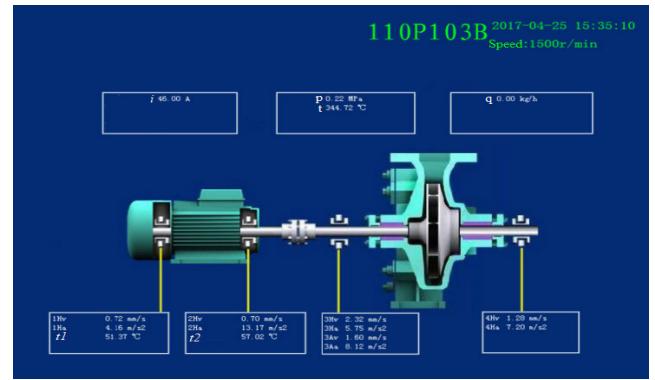


FIGURE 14. Schematic diagram of unit and measuring points.

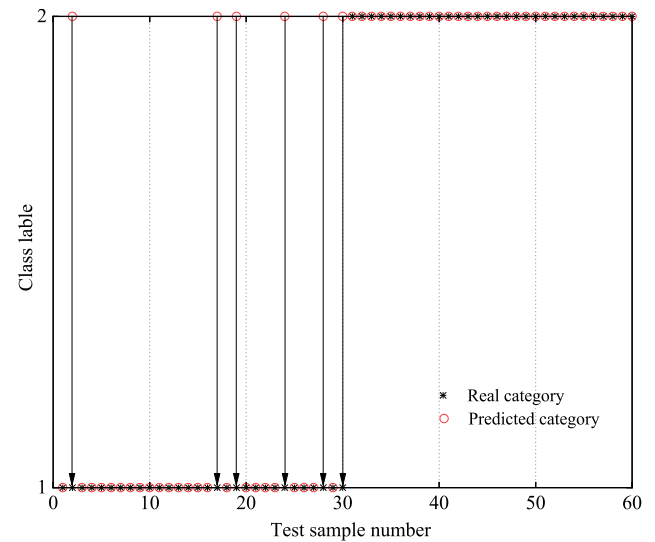


FIGURE 15. Test results of fault identification model based on 110P103B pump bearing data.

model is 6220 and the sampling frequency is 25600 Hz. Raw vibration data is filed every twenty minutes. The number of sampling points is 16384.

Raw acceleration data of the 110P103B pump was continuously obtained from 13:00 h on April 14, 2017 to 18:00 h on April 20, 2017. There are 710 data files in total, and each data file is composed of 16384 sampling points. Starting from April 17, 2017, the vibration acceleration trend slightly increased, and the vibration acceleration increased significantly on April 20 with the highest peak value rising to approximately  $88 m/s^2$ . A peeling in the inner ring of the pump free end bearing was observed during on-site shutdown and maintenance. It was contributed to a fault in the inner ring. The method in [39] is used to determine the data file of fault. Normal data without failure and the inner ring data following the failure are screened as the test set data. There are 30 sets of data for each bearing state. According to WOA algorithm, parameter results are adaptively adjusted and  $[K, \alpha] = [5, 2750]$  is obtained.

As shown in Fig. 15, fault identification accuracy rate is 90%, and there are six sets of normal data identification

errors. Due to relatively large noise interference of the engineering data and complicated working conditions when a fault occurs, the recognition accuracy rate has decreased.

## 2) P3409A PUMP BEARING DATASET BASED MODEL VALIDATION

This data represents a failure case of the drive end bearing of the petrochemical company's hydrocracking production unit P3409A pump. The layout of vibration monitoring points for pump bearings is shown in Fig. 16. Pump speed is 2980 r/min, the drive end bearing model is 6217, and the sampling frequency is 25600 Hz. Raw vibration data is acquisitioned every two hours. The number of sampling points for each group of data is 16384.

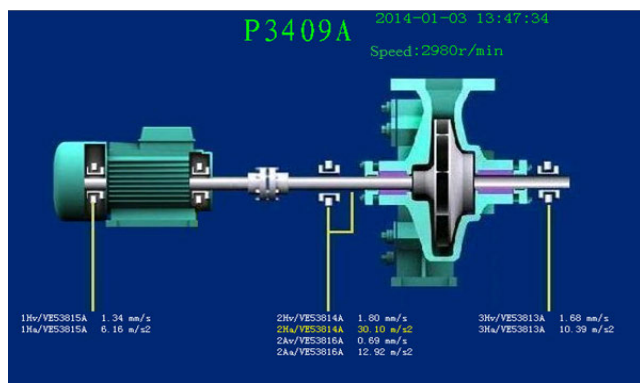


FIGURE 16. Schematic diagram of unit and measuring points [46].

Raw acceleration data of the P3409A pump was obtained from 24:00 h on December 15, 2013 to 16:00 h on January 12, 2014. There are 332 data files in total, and each data file consists of 16384 sampling points. From 12:16 h to 12:21 h on January 12, 2014, the vibration speed increased from 2.88 mm/s to 4.55 mm/s. This has triggered an alarm, and it was concluded that the outer bearing ring was faulty. The bearing performance degradation detection model constructed by Wang *et al.* [45] suggests that the 142<sup>nd</sup> data file is the starting point for bearing performance degradation. First confirmed failure data file is used as the first test sample, and normal data when no failure occurs and outer ring failure data following the failure are screened as the test set data. There are 30 sets of data for each bearing state. According to WOA algorithm adaptive adjustment, the result is obtained as  $[K, \alpha] = [5, 2900]$ .

As shown in Fig. 17, the recognition accuracy is 86.7%. However, it is still higher than 85%. According to the criteria given in Section III, for engineering data, the result can be regarded as credible. The above two sets of case data show that the model built on CWRU data is also effective in identifying engineering data.

Two sets of experimental data of IMS and MFPT and two sets of engineering data of 110P103B pump and P3409A pump are all performed in 10-fold cross-validation. The standard deviations of recognition accuracy are 1.1%, 1.8%,

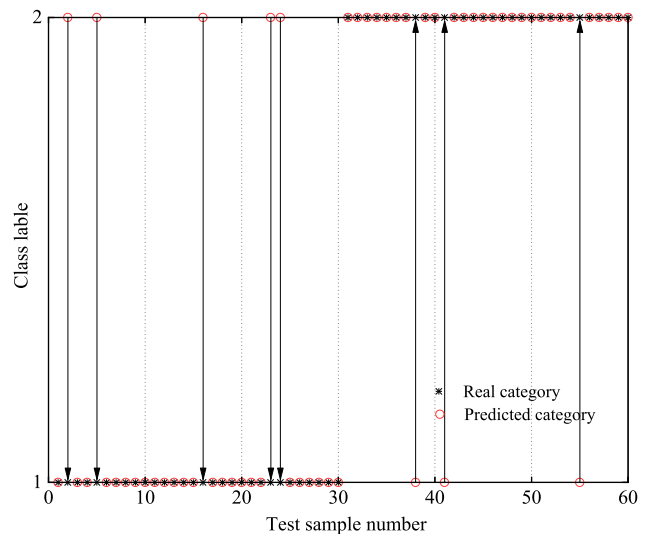


FIGURE 17. Test results of fault identification model based on P3409A pump bearing data.

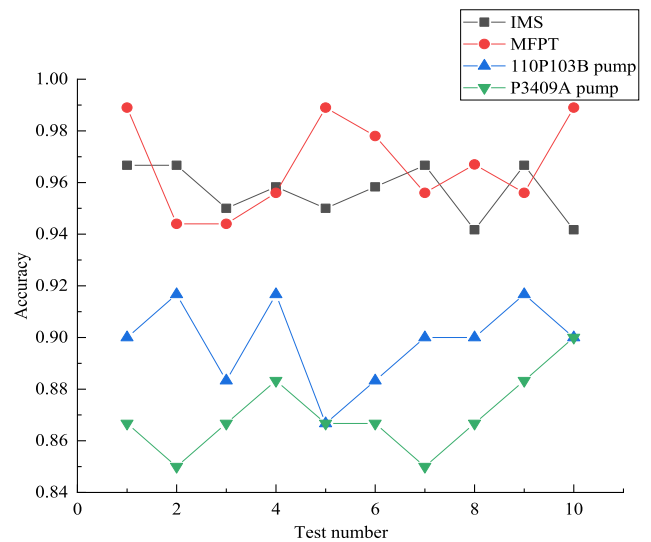


FIGURE 18. Accuracy curves based on experimental data and engineering data.

1.6% and 1.5%, respectively. The accuracy curves are shown in Fig. 18.

As shown in Fig. 18, the fault recognition accuracy of four sets of data is relatively stable and the standard deviation is small, which indicates that the model constructed in this paper has a good recognition effect on experimental data and engineering case data. This method provides a feasible way to identify the failure mode of rolling bearings across different working conditions of the equipment.

## D. METHOD COMPARISON

### 1) DIFFERENT FAULT FEATURE VECTORS

Automatic rolling bearing fault identification model proposed in this paper is applied, the differences in the identification



accuracy of five different fault feature vector values under the same model framework are compared. Sample entropy (SampEn), permutation entropy (PeEn), approximate entropy (ApEn), power spectrum entropy (PSE), and singular value entropy (SVE) are used to replace the refined composite multi-scale dispersion entropy within the model and calculate the eigenvector value of the reconstructed signal. A fault knowledge rule database, corresponding to each eigenvector value of the rolling bearing and the fault mode, is established when six different fault feature vector values are used as the input of the optimized SVM fault classifier. CWRU rolling bearing and IMS rolling bearing experimental data are used for validation. The recognition accuracy of the model is shown in Table 4. Experiments are all performed in 10-fold cross-validation, and the accuracy curves are shown in Fig. 19 and Fig. 20.

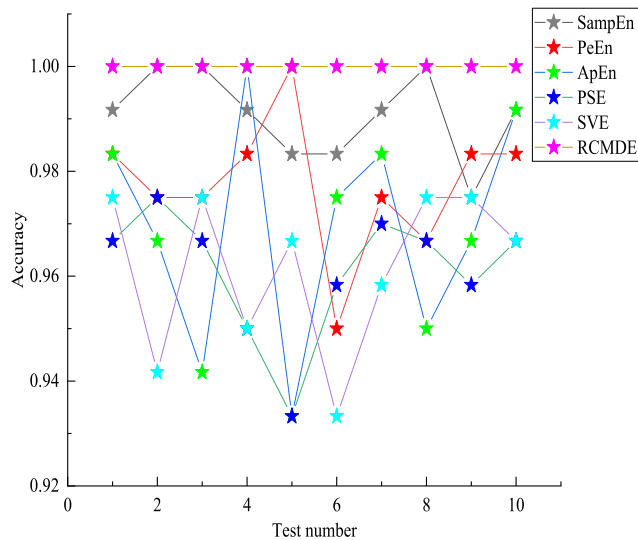


FIGURE 19. Accuracy curves based on CWRU data.

As shown in Table 4, automatic identification model test of rolling bearing failure mode is carried out based on CWRU data. When RCMDE feature vector value is used as the input of the optimized SVM fault classifier, the fault recognition accuracy of the model is the highest (it reaches 100%). Based on IMS data, automatic identification model test of rolling bearing failure mode is carried out. When RCMDE feature vector value is used as the input of the optimized SVM fault classifier, the model has the highest fault identification accuracy (96.67%). When SampEn, PeEn, ApEn, PSE, and SVE feature vector values are employed as the input of the optimized SVM fault classifier, the recognition accuracy of the model is 86.67%, 75.83%, 68.33%, 65%, and 56.67%, respectively.

The test data shows that, compared with the other five feature values, automatic identification model of rolling bearing failure modes based on RCMDE feature vector values has the highest recognition accuracy. As shown in Fig. 20, only when RCMDE as feature vector value, the built model has the best

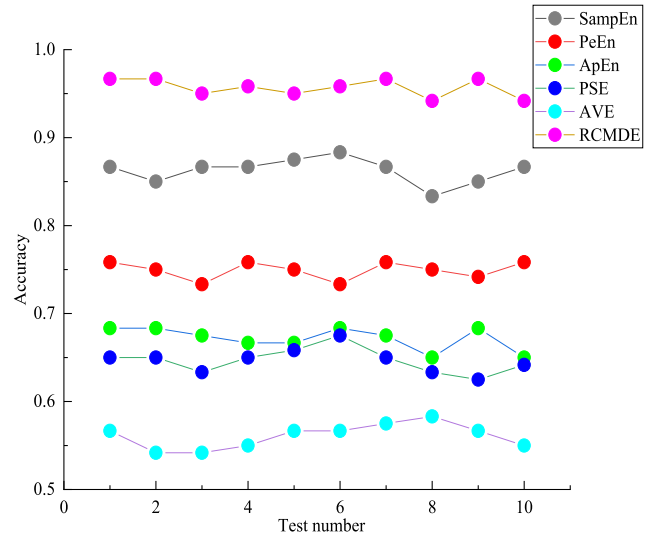


FIGURE 20. Accuracy curves based on IMS data.

TABLE 4. Model recognition accuracy corresponding to six different fault feature vector values.

Fault feature vector	Recognition accuracy(%)	
	Based on CWRU data	Based on IMS data
SampEn	99.17	86.67
PeEn	98.33	75.83
ApEn	98.33	68.33
PSE	96.67	65
SVE	97.5	56.67
RCMDE	100	96.67

fault identification effect on IMS data. Based on the model proposed in this paper, RCMDE as a feature value can better characterize the failure characteristics of rolling bearings under different equipment and operating environment, and has better generalization performance.

## 2) DIFFERENT FAULT IDENTIFICATION MODELS

As mentioned above, good performance of RCMDE as a feature value has been verified. In order to further show superiority of the model proposed in this paper, four different fault recognition models are employed in this section to compare with this built model: fault identification model based on weighted k-nearest neighbor (WKNN) classifier (Model 1), fault identification model based on decision tree classifier (Model 2), fault identification model based on CNN (Model 3) and fault identification model based on Naive Bayesian classifier (Model 4). In Model 1, WKNNC is used to classify the extracted RCMDE feature values, the nearest neighbor  $k$  value is 10. In Model 2, RCMDE value and decision tree are applied to fault identification, the maximum split value is 100. In Model 3, a CNN model of double convolutional layer is employed to identify the failure mode of the original vibration data. In Model 4, RCMDE and Naive Bayesian classifier based on Gaussian kernel are used for fault identification.

The same experimental data of CWRU rolling bearing and IMS rolling bearing as above are used for verification, a 10-fold cross-validation process is executed, and the average recognition accuracy of these models can be shown in Table 5.

**TABLE 5. Model recognition accuracy corresponding to five different models.**

Comparison model	Recognition accuracy (%)	
	Based on CWRU data	Based on IMS data
Model 1	97.4	90
Model 2	94.9	87.5
Model 3	96.6	45.2
Model 4	98.9	92
Model of this paper	100	96.67

As shown in Table 5, The fault recognition accuracy of Model 1, Model 2, Model 3 and Model 4 based on CWRU data are 97.4%, 94.9%, 96.6% and 98.9%, respectively. The fault recognition accuracy based on IMS data are 90%, 87.5%, 45.2% and 92%. The model constructed in this paper has the highest fault recognition accuracy for CWRU data and IMS data, which indicates that the model has certain advantages in fault recognition.

### 3) METHOD PROPOSED IN PAPER [20]

An overview of the rolling bearing failure mode recognition method based on VMD and energy entropy feature vector value of LSSVM is presented in this section [20].

Step 1: The wavelet threshold de-noising method is used to preprocess the rolling bearing vibration signal.

Step 2: The genetic algorithm is used to optimize VMD parameters (penalty factor  $\alpha$  and decomposition level  $K$ ). VMD algorithm is employed to adaptively decompose raw vibration bearing signal into a series of modal components.

Step 3: Fault feature components are screened. Energy entropy of the reconstructed signal is calculated to form a feature vector matrix.

Step 4: Based on the training data set under various working conditions, knowledge rule database of one-to-one correspondence between energy entropy value and rolling bearing failure mode is established.

Step 5: Optimized LSSVM is used to classify and identify failure modes of bearings.

The model training data uses CWRU rolling bearing data set, which includes 120 sets of normal state data, outer ring failure, inner ring failure, and rolling element failure training data under different operating speeds and applied loads. A total of 30 sets of rolling bearing normal state, bearing outer ring failure, inner ring failure, and rolling element failure data under different operating speeds and applied loads are screened as the test data set.

As shown in Fig. 21 and Fig. 22, the rolling bearing fault identification model based on optimized VMD, optimized LSSVM and feature vector energy entropy is tested using CWRU data set, with the corresponding accuracy

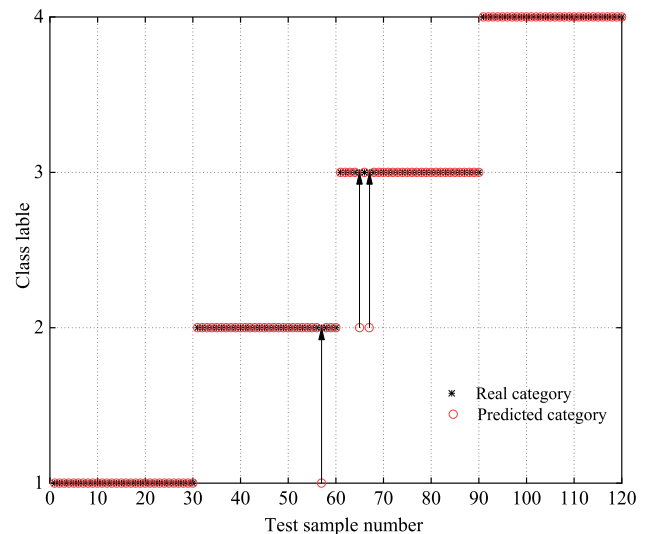


**FIGURE 21. Test results of fault identification model based on CWRU data by using method [20].**

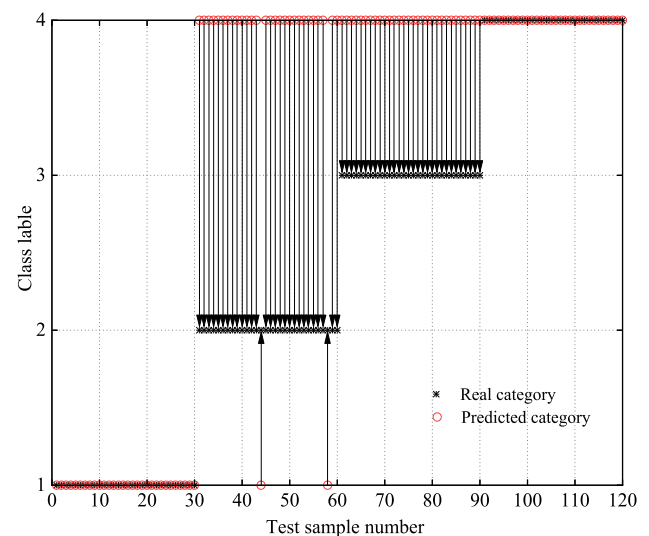


**FIGURE 22. Test results of fault identification model based on IMS data by using method [20].**

being 97.5%. The IMS data set is utilized to test the recognition accuracy of rolling bearings, which is equal to only 50%. When model training data and test data share the same source, the model has a higher fault recognition accuracy. Otherwise, fault recognition accuracy of the model is relatively low, and it is basically inapplicable in engineering. Comparative analysis shows that generalization of the failure mode identification model is relatively poor.

### 4) METHOD PROPOSED IN PAPER [29]

SVM rolling bearing fault pattern recognition method with IEWT and RCMDE feature vector value is summarized in this section [29].

Step 1: IEWT algorithm is used to decompose the original bearing vibration signal into a series of modal components.

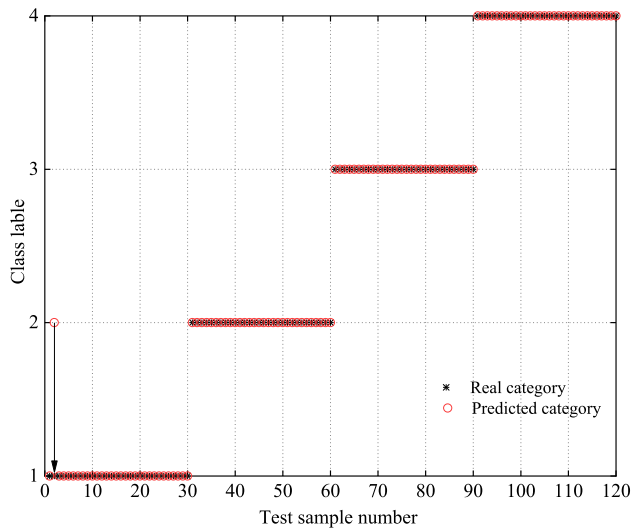


FIGURE 23. Test results of fault identification model based on CWRU data by using method [29].

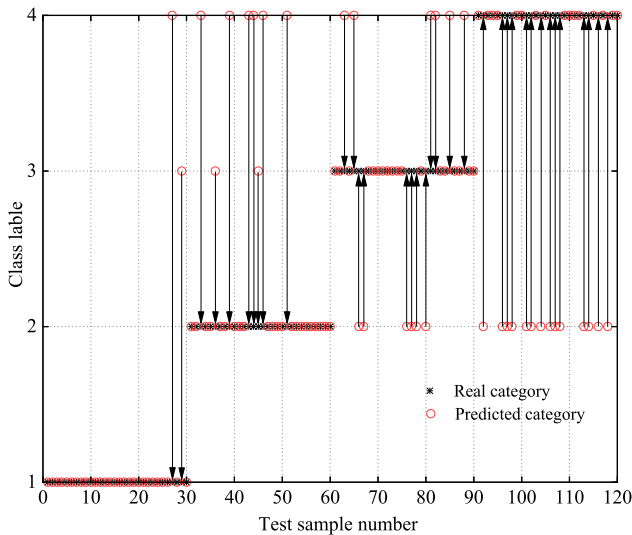


FIGURE 24. Test results of fault identification model based on IMS data by using method [29].

Step 2: The RCMDE of each component obtained by IEWT is computed and form feature matrix.

Step 3: Multi-cluster feature selection is used to select features as sensitive feature.

Step 4: The sensitive features are input to the SVM for training, and the testing by the trained classifier model.

Fault identification model of rolling bearing based on IEWT and RCMDE feature vector values is presented in Fig. 23 and Fig. 24. CWRU data set is employed for testing, and rolling bearing fault identification accuracy rate is 99.17%. When IMS data set is employed, fault identification accuracy rate is only 70%. When the model training data and test data share the same source, the model has a higher fault recognition accuracy. On the contrary, fault recognition accuracy of the model is relatively low and it is virtually impossible to use it for engineering applications.

TABLE 6. Model recognition accuracy corresponding to three different methods.

Comparison method	Recognition accuracy (%)	
	Based on CWRU data	Based on IMS data
Method in [20]	97.5	50
Method in [29]	99.17	70
Method of this paper	100	96.67

Moreover, comparative analysis shows that the failure mode identification model has poor generalization.

As shown in Table 6, the method proposed in this paper has better fault recognition accuracy. This method uses improved VMD to decompose the vibration signal into a series of IMF components. Correlation coefficient method is used for screening and signal reconstruction. RCMDE value of the reconstructed signal is calculated and input into the optimized SVM classifier. Recognition accuracy of the proposed method is significantly higher than that of the other two methods, especially for the IMS equipment data. This provides a feasible way for the identification of rolling bearing failure modes under different operating conditions. Rolling bearing fault automatic identification model based on RCMDE value proposed in this paper shows good fault identification accuracy both experimental data and typical engineering case data.

## V. CONCLUSION

1) In this paper, rolling bearing online fault mode automatic identification model is constructed and a generalized method for constructing fault identification model based on RCMDE is proposed. Model input is the raw vibration time series data, while its output is rolling bearing fault identification conclusion. The maximum kurtosis method is proposed to solve the problem that value range of decomposition layer  $K$  preset relying on prior knowledge when WOA algorithm is used to optimized VMD. The key parameters in VMD and SVM are optimized to make it more reasonable for different rolling bearing data in the model proposed in this paper. There is no need to rely on the experience of external experts in the working mode, and it can be applied to rolling bearings under different equipment or operating environment to a certain extent.

2) Using the method proposed in this paper, the feature vectors such as SampEn, PeEn, ApEn, PSE, SVE, RCMDE are selected to construct the corresponding models respectively. The accuracy of fault recognition based on CWRU data is respectively 99.17%, 98.33%, 98.33%, 96.67%, 97.5% and 100%. The accuracy of fault recognition based on IMS data is respectively 86.67%, 75.83%, 68.33%, 65%, 56.67% and 96.67%. It can be seen from the above that the fault recognition model based on RCMDE value has better recognition accuracy.

3) Based on the training data set under various working conditions, a knowledge rule database of one-to-one correspondence is established between RCMDE values and rolling

bearing failure modes. The remaining part of CWRU data set, IMS data set, MFPT data set, 110P103B pump bearing fault case data set, and P3409A pump bearing fault case data set are used for the model testing. The fault automatic identification accuracy rate of the constructed model in this paper reached 100%, 96.67%, 98.9%, 90% and 86.7%, respectively. Data verification results indicate that the constructed model has high recognition accuracy for different equipment and operating conditions. Comparisons with different fault identification models and with different fault diagnosis methods, superiority of the model constructed in this paper is proved.

## REFERENCES

- [1] K. T. P. Nguyen and K. Medjaher, "A new dynamic predictive maintenance framework using deep learning for failure prognostics," *Rel. Eng. Syst. Saf.*, vol. 188, pp. 251–262, Aug. 2019.
- [2] M. Kordestani, M. Saif, M. E. Orchard, R. Razavi-Far, and K. Khorasani, "Failure prognosis and applications—A survey of recent literature," *IEEE Trans. Rel.*, vol. 70, no. 2, pp. 728–748, Jun. 2021, doi: 10.1109/TR.2019.2930195.
- [3] Q. Wang, J. Liu, B. Wei, W. Chen, and S. Xu, "Investigating the construction, training, and verification methods of k-means clustering fault recognition model for rotating machinery," *IEEE Access*, vol. 8, pp. 196515–196528, 2020.
- [4] C.-W. Fei, Y.-S. Choy, G.-C. Bai, and W.-Z. Tang, "Multi-feature entropy distance approach with vibration and acoustic emission signals for process feature recognition of rolling element bearing faults," *Struct. Health Monitor.*, vol. 17, no. 2, pp. 156–168, Mar. 2018.
- [5] H. Lin, F. Wu, and G. He, "Rolling bearing fault diagnosis using impulse feature enhancement and nonconvex regularization," *Mech. Syst. Signal Process.*, vol. 142, Aug. 2020, Art. no. 106790, doi: 10.1016/j.ymssp.2020.106790.
- [6] Z. Meng, X. Zhan, J. Li, and Z. Pan, "An enhancement denoising autoencoder for rolling bearing fault diagnosis," *Measurement*, vol. 130, pp. 448–454, Dec. 2018.
- [7] Z. Chen, J. Cen, and J. Xiong, "Rolling bearing fault diagnosis using time-frequency analysis and deep transfer convolutional neural network," *IEEE Access*, vol. 8, pp. 150248–150261, 2020.
- [8] Y. Zhang, T. Shu, C. Liu, and R. Ding, "Rolling bearing fault diagnosis based on GUI system," *J. Phys., Conf. Ser.*, vol. 1754, no. 1, Feb. 2021, Art. no. 012138, doi: 10.1088/1742-6596/1754/1/012138.
- [9] Y. Shi, A. Deng, M. Deng, J. Zhu, Y. Liu, and Q. Cheng, "Enhanced lightweight multiscale convolutional neural network for rolling bearing fault diagnosis," *IEEE Access*, vol. 8, pp. 217723–217734, 2020.
- [10] Y. Miao, M. Zhao, and J. Hua, "Research on sparsity indexes for fault diagnosis of rotating machinery," *Measurement*, vol. 158, Jul. 2020, Art. no. 107733, doi: 10.1016/j.measurement.2020.107733.
- [11] Y. Miao, M. Zhao, K. Liang, and J. Lin, "Application of an improved MCKDA for fault detection of wind turbine gear based on encoder signal," *Renew. Energy*, vol. 151, pp. 192–203, May 2020, doi: 10.1016/j.renene.2019.11.012.
- [12] J. L. Jiang, W. Y. Liu, Y. J. Hou, Z. M. Zhong, and S. Y. Chen, "Bearing fault diagnosis based on integral waveform extension LMD and SVM," *J. Vibrot. Shock*, vol. 35, no. 6, pp. 104–108, 2016.
- [13] S. Luo, W. Yang, and Y. Luo, "A novel fault detection scheme using improved inherent multiscale fuzzy entropy with partly ensemble local characteristic-scale decomposition," *IEEE Access*, vol. 8, pp. 6650–6661, 2020.
- [14] G. Xian, "Parallel machine learning algorithm using fine-grained-mode spark on a mesos big data cloud computing software framework for mobile robotic intelligent fault recognition," *IEEE Access*, vol. 8, pp. 131885–131900, 2020.
- [15] S. J. Dong, X. W. Pei, W. L. Wu, B. P. Tang, and X. X. Zhao, "Rolling bearing fault diagnosis method based on multilayer noise reduction technology and improved convolutional neural network," *J. Mech. Eng.*, vol. 57, no. 1, pp. 148–156, 2021.
- [16] K. Dragomiretskiy and D. Zosso, "Variational mode decomposition," *IEEE Trans. Signal Process.*, vol. 62, no. 3, pp. 531–544, Feb. 2014.
- [17] Y. Q. Song, S. C. Deng, and Y. G. Lu, "Application of k value optimized VMD in bearing fault diagnosis," *Meas. Control Technol.*, vol. 38, no. 4, pp. 117–121, 2019.
- [18] J. Ding, D. Xiao, and X. Li, "Gear fault diagnosis based on genetic mutation particle swarm optimization VMD and probabilistic neural network algorithm," *IEEE Access*, vol. 8, pp. 18456–18474, 2020.
- [19] C. Wang, H. Li, G. Huang, and J. Ou, "Early fault diagnosis for planetary gearbox based on adaptive parameter optimized VMD and singular kurtosis difference spectrum," *IEEE Access*, vol. 7, pp. 31501–31516, 2019.
- [20] J. Li, W. Chen, K. Han, and Q. Wang, "Fault diagnosis of rolling bearing based on GA-VMD and improved WOA-LSSVM," *IEEE Access*, vol. 8, pp. 166753–166767, 2020.
- [21] J. D. Zheng, H. Y. Pan, J. S. Cheng, and J. Zhang, "Composite multi-scale fuzzy entropy based rolling bearing fault diagnosis method," *J. Vibrot. Shock*, vol. 35, no. 8, pp. 116–123, 2016.
- [22] C. Li, J. Zheng, H. Pan, J. Tong, and Y. Zhang, "Refined composite multivariate multiscale dispersion entropy and its application to fault diagnosis of rolling bearing," *IEEE Access*, vol. 7, pp. 47663–47673, 2019.
- [23] D. Han, X. Guo, and P. Shi, "An intelligent fault diagnosis method of variable condition gearbox based on improved DBN combined with WPEE and MPE," *IEEE Access*, vol. 8, pp. 131299–131309, 2020.
- [24] Y. Li, X. Wang, Z. Liu, and S. Si, "A fault diagnosis method of planetary gearbox under variable speed condition using Vold-Kalman filter and Laplacian score," in *Proc. IEEE Int. Conf. Prognostics Health Manage. (ICPHM)*, Jun. 2018, pp. 1–5, doi: 10.1109/ICPHM.2018.8448875.
- [25] C. He, T. Wu, R. Gu, Z. Jin, R. Ma, and H. Qu, "Rolling bearing fault diagnosis based on composite multiscale permutation entropy and reverse cognitive fruit fly optimization algorithm—Extreme learning machine," *Measurement*, vol. 173, Mar. 2021, Art. no. 108636, doi: 10.1016/j.measurement.2020.108636.
- [26] M. Rostaghi and H. Azami, "Dispersion entropy: A measure for time-series analysis," *IEEE Signal Process. Lett.*, vol. 23, no. 5, pp. 610–614, May 2016.
- [27] H. Azami, M. Rostaghi, D. Abásolo, and J. Escudero, "Refined composite multiscale dispersion entropy and its application to biomedical signals," *IEEE Trans. Biomed. Eng.*, vol. 64, no. 12, pp. 2872–2879, Dec. 2017.
- [28] X. Zhang, J. Zhao, H. Teng, and G. Liu, "A novel faults detection method for rolling bearing based on RCMDE and ISVM," *J. Vibroeng.*, vol. 21, no. 8, pp. 2148–2158, Dec. 2019.
- [29] J. Zheng, S. Huang, H. Pan, and K. Jiang, "An improved empirical wavelet transform and refined composite multiscale dispersion entropy-based fault diagnosis method for rolling bearing," *IEEE Access*, vol. 8, pp. 168732–168742, 2020.
- [30] C. Z. Li, J. D. Zheng, H. Y. Pan, and Q. Y. Liu, "Fault diagnosis method of rolling bearings based on refined composite multiscale dispersion entropy and support vector machine," *China Mech. Eng.*, vol. 30, no. 14, pp. 1713–1719, 2019.
- [31] C. W. Fei, H. Li, H. T. Liu, C. Lu, L. Q. An, and L. Han, "Enhanced network learning model with intelligent operator for the motion reliability evaluation of flexible mechanism," *Aerosp. Sci. Technol.*, vol. 297, pp. 1–11, Dec. 2020, doi: 10.1016/j.ast.2020.106342.
- [32] J. Feng, J. Liu, and H. Zhang, "Speed control of pipeline inner detector based on interval dynamic matrix control with additional margin," *IEEE Trans. Ind. Electron.*, early access, Dec. 31, 2021, doi: 10.1109/TIE.2020.3047061.
- [33] C. W. Fei, H. Li, H. T. Liu, C. Lu, and B. Keshtegar, "Multilevel nested reliability-based design optimization with hybrid intelligent regression for operating assembly relationship," *Aerosp. Sci. Technol.*, vol. 285, pp. 1–11, Aug. 2020, doi: 10.1016/j.ast.2020.105906.
- [34] J. Liu, J. Feng, and X. Gao, "Fault diagnosis of rod pumping wells based on support vector machine optimized by improved chicken swarm optimization," *IEEE Access*, vol. 7, pp. 171598–171608, 2019.
- [35] F. Jiang, Z. Zhu, and W. Li, "An improved VMD with empirical mode decomposition and its application in incipient fault detection of rolling bearing," *IEEE Access*, vol. 6, pp. 44483–44493, 2018.
- [36] S. Mirjalili and A. Lewis, "The whale optimization algorithm," *Adv. Eng. Softw.*, vol. 95, pp. 51–67, May 2016.
- [37] C. Cortes and V. Vapnik, "Support-vector networks," *Mach. Learn.*, vol. 20, no. 3, pp. 273–297, 1995.
- [38] Y. Wang, D. Wang, and Y. Tang, "Clustered hybrid wind power prediction model based on ARMA, PSO-SVM, and clustering methods," *IEEE Access*, vol. 8, pp. 17071–17079, 2020.



- [39] Q. Wang, X. Liu, B. Wei, and W. Chen, "Online incipient fault detection method based on improved  $\ell_1$  trend filtering and support vector data description," *IEEE Access*, vol. 9, pp. 30043–30059, 2021.
- [40] J. D. Zheng, "Research on local characteristic-scale decomposition and its applications to machinery fault diagnosis," Ph.D. dissertation, Dept. Mecha. Eng., Hunan Univ, Changsha, China, 2014.
- [41] (2013). *Bearing Data Center*. [Online]. Available: <https://csegroups.case.edu/bearingdatacenter/home>
- [42] Q. Wang, S. Wang, B. Wei, W. Chen, and Y. Zhang, "Weighted K-NN classification method of bearings fault diagnosis with multi-dimensional sensitive features," *IEEE Access*, vol. 9, pp. 45428–45440, 2021.
- [43] (2014). *IMS Bearings Dataset*. [Online]. Available: <http://ti.arc.nasa.gov/tech/dash/pcoe/prognostic-data-repository/>
- [44] E. Bechhoefer. (2016). *A Quick Introduction to Bearing Envelope Analysis, MFPT Data*. [Online]. Available: <http://www.mfpt.org/FaultData/Fault-Data.htm.Set>
- [45] Q. F. Wang, B. K. Wei, J. H. Liu, W. S. Ma, and S. J. Xu, "Research on construction and application of data-driven incipient fault detection model for rotating machinery," *J. Mech. Eng.*, vol. 56, no. 16, pp. 22–32, 2020.
- [46] Q. Wang, B. Wei, J. Liu, and W. Ma, "Data-driven incipient fault prediction for non-stationary and non-linear rotating systems: Methodology, model construction and application," *IEEE Access*, vol. 8, pp. 197134–197146, 2020.



**YANG XIAO** received the B.S. degree from the College of Chemical Engineering, China University of Mining and Technology, China, in 2020, where he is currently pursuing the M.S. degree. His current research interest includes fault diagnosis.



**SHUAI WANG** received the B.S. degree from the College of Chemical Engineering, China University of Mining and Technology, China, in 2019, where he is currently pursuing the M.S. degree. His current research interest includes fault diagnosis.



**WENCAI LIU** is a Senior Engineer working with the CNPC Research Institute of Safety and Environment Technology. He has been engaged in equipment safety technology research. His research interests include electromechanical equipment monitoring, diagnosis, and maintenance.



**XIAOJIN LIU** received the B.S. degree from the College of Mechanical Engineering, North China University of Science and Technology, China, in 2019, where he is currently pursuing the M.S. degree. His current research interests include incipient fault warning and health evaluation.

...



**QINGFENG WANG** received the Ph.D. degree from the College of Mechanical and Electrical Engineering, Beijing University of Chemical Technology, China, in 2011. He is currently an Associate Researcher with the College of Mechanical and Electrical Engineering, Beijing University of Chemical Technology. He is also a Security Expert of the State Administration of Work Safety of China. His research interests include electromechanical equipment monitoring, diagnosis, and maintenance.